An Epitaxial Transparent Conducting Perovskite Oxide: Double-Doped $SrTiO_3$

Jayakanth Ravichandran,*,[†] Wolter Siemons,[‡] Herman Heijmerikx,[‡,§]
Mark Huijben,[§] Arun Majumdar,[∥] and Ramamoorthy Ramesh[‡,⊥]

*Applied Science and Technology Graduate Group, University of California, Berkeley California 94720,
Department of Physics, University of California, Berkeley California 94720, Faculty of Science and
Technology, University of Twente, P. O Box 217, 7500 AE, Enschede (The Netherlands), Advanced Research
Projects Agency − Energy, U.S. Department of Energy, Washington, DC 20585, and Department of
Materials Science and Engineering, University of California, Berkeley California 94720. [†]Applied Science
and Technology Graduate Group, University of California. [‡]Department of Physics, University of
California. [§]University of Twente. [∥]Department of Energy. [⊥]Department of Materials Science and
Engineering, University of California.*

Received February 23, 2010. Revised Manuscript Received May 11, 2010

Epitaxial thin films of strontium titanate doped with different concentrations of lanthanum and oxygen vacancies were grown on LSAT substrates by pulsed laser deposition technique. Films grown with 5−15% La doping and a critical growth pressure of 1−10 mTorr showed high transparency (>70−95%) in the UV−visible range with a sheet resistance of 300−1000 $\Omega/\square$. With the aid of UV−visible spectroscopy and photoluminescence, we establish the presence of oxygen vacancies and the possible band structure, which is crucial for the transparent conducting nature of these films. This demonstration will enable development of various epitaxial oxide heterostructures for both realizing opto-electronic devices and understanding their intrinsic optical properties.

Introduction

Transparent conducting oxides (TCOs) are an interesting class of materials which combine two conflicting properties, namely electrical conduction and optical transparency. The guiding principle in designing a transparent conductor is the creation of defect levels close to conduction or valence bands of a wide band gap semiconductor. Ionization of these defects produces a degenerate electron gas causing only free carrier absorption in far-infrared regime but maintains good optical transparency in the UV−visible region by retaining the band gap of the material.[1] Perovskite oxides show a wide range of exotic phenomena namely superconductivity,[2] thermoelectricity,[3] and colossal magneto-resistance.[4] However, there are very few reports of transparent conducting perovskite oxides, most notably $In_xCd_3TeO_6$,[5] Sb-doped $SrSnO_3$,[6] $ZnSnO_3$,[7] La- and Sb-doped $BaSnO_3$,[8] and Cd−In−Sn−O.[9] $SrTiO_3$ (STO) is a model functional perovskite oxide and widely used as substrate material for the growth of oxide thin films. It has a wide band gap and can be easily doped on cationic sites or with oxygen vacancies. Heavy doping of STO using La or Nb has been demonstrated in both bulk[10] and thin films,[11] leading to metallic conductivities. In the past, efforts have been made to produce a transparent conducting oxide using STO by tuning the oxygen vacancies in amorphous or polycrystalline films[12] or antimony (Sb) doping[13] with no significant success. Recently, it was discovered that a very thin surface layer (1−3 nm) of STO becomes conducting by Ar ion bombardment while maintaining excellent transparency, presumably due to oxygen vacancies.[14] Another report on $La_{0.5}Sr_{0.5}TiO_{3+\delta}$[15]

---

*Author to whom correspondence should be addressed. Tel.: +1-510-643-8202. Fax +1-510-643-5792. E-mail: jayakanth@berkeley.edu.

(1) Edwards, P. P.; Porch, A.; Jones, M. O.; Morgan, D. V.; Perks, R. M. *Dalton Trans.* **2004,** 2995.
(2) Schooley, J. F.; Hosler, W. R.; Cohen, M. L. *Phys. Rev. Lett.* **1964,** *12,* 474.
(3) Frederikse, H. P. R.; Thurber, W. R.; Hosler, W. R. *Phys. Rev.* **1964,** *134,* A442.
(4) Jin, S.; Tiefel, T. H.; McCormack, M.; Fastnacht, R. A.; Ramesh, R.; Chen, L. H. *Science* **1994,** *264,* 413.
(5) Tetsuka, H.; Shan, Y. J.; Tetsuka, K.; Imoto, H.; Wasa, K. *J. Mater. Res.* **2005,** *20,* 2256.
(6) Liu, Q. Z.; Wang, H. F.; Chen, F.; Wu, W. *J. Appl. Phys.* **2008,** *103,* 093709.
(7) Minami, T.; Sonohara, H.; Takata, S.; Sato, H. *Jpn. J. Appl. Phys.* **1994,** *33,* L1693.
(8) Wang, H. F.; Liu, Q. Z.; Chen, F.; Gao, G. Y.; Wu, W.; Chen, X. H. *J. Appl. Phys.* **2007,** *101,* 106105.
(9) Mason, T. O.; Kammler, D. R.; Ingram, B. J.; Gonzalez, G. B.; Young, D. L.; Coutts, T. J. *Thin Solid Films* **2003,** *445,* 186.
(10) Ohta, S.; Nomura, T.; Ohta, H.; Koumoto, K. *J. Appl. Phys.* **2005,** *97,* 034106.
(11) Ohta, S.; Nomura, T.; Ohta, H.; Hirano, M.; Hosono, H.; Koumoto, K. *Appl. Phys. Lett.* **2005,** *87,* 092108.
(12) Campet, G.; Geoffroy, C.; Manaud, J. P.; Portier, J.; Sun, Z. W.; Salardenne, J.; Keou, P. *Mater. Sci. Eng. B* **1991,** *8,* 45.
(13) Wang, H. H.; Chen, F.; Dai, S. Y.; Zhao, T.; Lu, H. B.; Cui, D. F.; Zhou, Y. L.; Chen, Z. H.; Yang, G. Z. *Appl. Phys. Lett.* **2001,** *78,* 1676.
(14) Reagor, D. W.; Butko, V. Y. *Nat. Mater.* **2005,** *4,* 593.
(15) Cho, J. H.; Cho, H. J. *Appl. Phys. Lett.* **2001,** *79,* 1426.

speculated the role of oxygen content in controlling the filling in Ti-3d states and hence the transparent conducting nature of La doped STO at the Mott−Hubbard limit (La doping ≫ 20%). These reports and theoretical predictions of a defect band formation due to oxygen vacancies in STO[16,17] suggest oxygen vacancies can be crucial for creating a TCO of doped STO. A doped STO based TCO will have far reaching implications in fabricating optoelectronics devices, for example photo detectors, solar cells, and light emitting diodes (LED) based on epitaxial perovskite oxide heterostructures, and also a single crystalline transparent bottom electrode will be crucial to understand the optoelectronic properties of such perovskite heterostructures. It is important to note that STO substrate has been the preferred substrate for a variety of single crystalline epitaxial perovskite heterostructures and a functional transparent conducting layer of doped STO can be easily integrated into such heterostructures. In this article, we report a heteroepitaxial TCO based on doped STO and establish the role of oxygen vacancies under the simple band picture using optical spectroscopy and transport measurements.

Experimental Section

Thin films of double-doped STO ($La_xSr_{1-x}TiO_{3-\delta}$, $x = 0-0.15$) were grown on $(LaAlO_3)_{0.3}-(Sr_2AlTaO_6)_{0.7}$ (LSAT) substrates ($<$1% lattice mismatch with bulk STO) using pulsed laser deposition (PLD). An excimer laser ($\lambda = 248$ nm) with laser fluence of 1.5 J cm^{-2} per pulse and repetition rate of 8 Hz was used to ablate commercial polycrystalline STO targets with nominal La doping of 0, 10, and 15%. The substrate temperature was maintained at 850 °C during the deposition. X-ray diffraction (XRD) was carried out on these films with a Panalytical X'Pert Pro thin film diffractometer using Cu Kα radiation. Low temperature resistivity and Hall measurements were performed in Van der Pauw geometry using a Quantum Design physical property measurement system (PPMS). Thermopower measurements at room temperature were done using a home-built setup with T type thermocouples. UV−visible transmission and reflection measurements were obtained from a Perkin-Elmer Lambda 950 spectrometer and Hitachi U-3010 spectrometer, respectively. The photoluminescence (PL) data were acquired using a setup with a 325 nm laser excitation source.

Results and Discussion

The electrical properties of the grown films can be tuned from insulating to metallic based on the La doping and growth pressure. It was observed that a critical amount of La doping and oxygen vacancies are required for producing a TCO and at the extreme limits of oxygen vacancies, STO acts either as an insulator (very high growth pressure or low oxygen vacancies) or a nontransparent metallic conductor (very low growth pressure or high oxygen vacancies). Figure 1 shows 150 nm thick films of doped STO which are (a) insulating (0% La
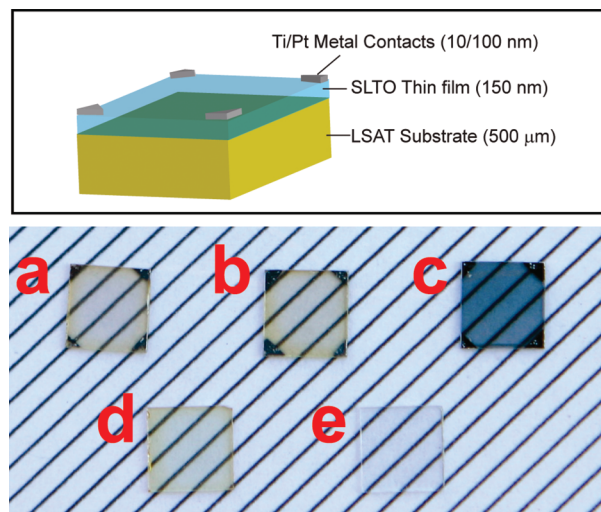

Figure 1. Schematic of sample structure is shown on top. Typically 150 nm thick STO film was grown on a 0.5 mm thick LSAT substrate and Ti/Pt contacts with 10/100 nm thicknesses were deposited for transport measurements in Van der Pauw geometry. Below is the photograph of STO thin films on LSAT substrate which are (a) transparent and insulating (0% La grown at 10^{-3} Torr), (b) transparent and conducting (15% La grown at 10^{-3} Torr), (c) nontransparent and conducting (15% La grown at 10^{-7} Torr), (d) bare LSAT substrate, and (e) bare MgO substrate.

grown at 10^{-3} Torr), (b) transparent and conducting (15% La grown at 10^{-3} Torr), and (c) nontransparent and conducting (15% La grown at 10^{-7} Torr). Substrates of (d) LSAT and (e) magnesium oxide (MgO) are shown for comparison. The inset of Figure 1 shows the schematic of the device structure used for the transport and optical spectroscopic measurements.

Figure 2 shows the X-ray diffraction (XRD) pattern for the transparent conducting sample grown at 10^{-3} Torr with 15% La doping. The diffraction pattern clearly demonstrates the absence of any secondary phase. The inset shows the rocking curve with full-width-at-half-maximum (fwhm) of ∼0.12°, indicating the high quality nearly single crystalline nature of the film. The out of plane lattice parameter for the TCO films was ∼3.926−3.934 Å and the reciprocal space map (not shown here) showed that all the films were strained in-plane to approximately the bulk STO's lattice parameter (3.905 Å). The observed tetragonal distortion is a clear signature of oxygen vacancies as predicted by earlier theoretical calculations.[16,18] Rutherford backscattering measurements show that the films contain the nominal 15% of La substituting Sr sites, maintaining a (La + Sr)/Ti ∼ 1. RBS-channeling experiments on the films confirmed the single crystalline nature, as observed by the rocking curve measurements. Even though it will be interesting to learn about the relationship between oxygen vacancy concentration and growth pressure using RBS, due to the limited sensitivity for vacancies of lighter atoms like oxygen, a reliable estimation of oxygen vacancy concentration cannot be made.

The transmission of the various doped thin films of STO (corrected for the absorption of the substrate) over

(16) Luo, W.; Duan, W.; Louie, S. G.; Cohen, M. L. *Phys. Rev. B.* **2004**, *70*, 214109.

(17) Wunderlich, W.; Ohta, H.; Kuomoto, K. *Physica B* **2009**, *404*, 2202.

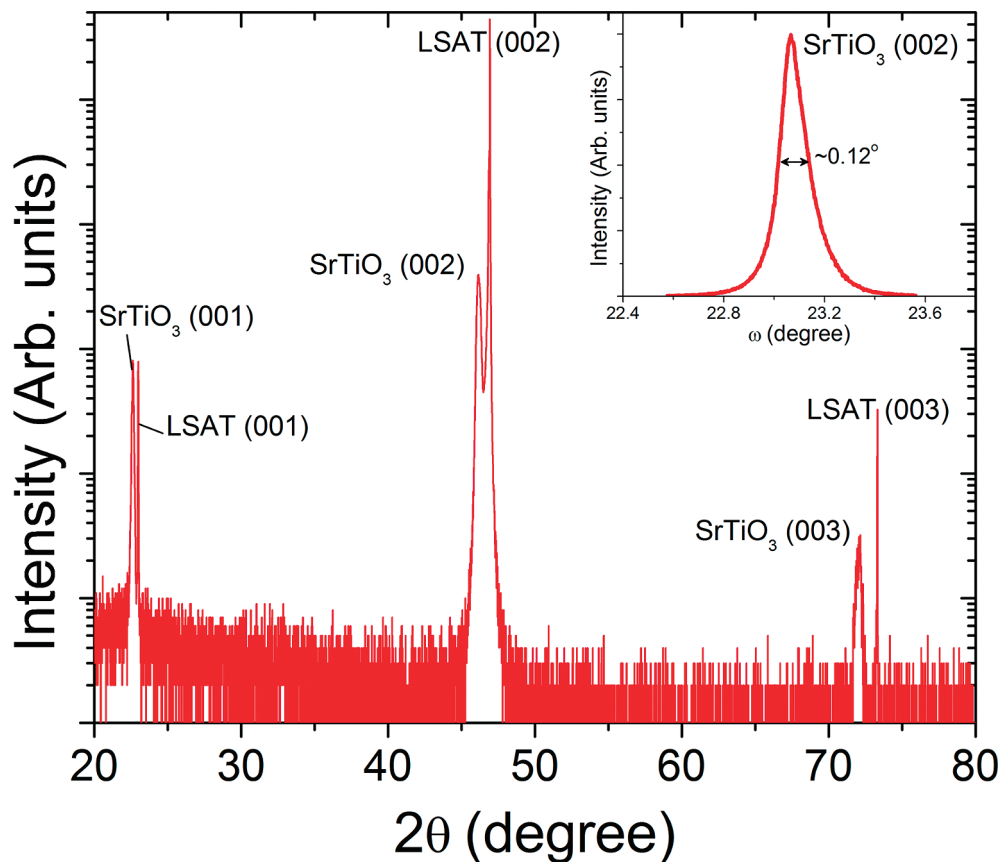(18) Astala, R.; Bristowe, P. D. *Comput. Mater. Sci.* **2001**, *22*, 81.

Figure 2. Thin film X-ray diffraction pattern of 15% La doped STO film grown at 10^{-3} Torr (marked as SrTiO$_3$). The pattern shows only peaks corresponding to strained STO thin film apart from the substrate peaks (marked as LSAT). The inset shows the rocking curve for the (002) peak of the STO thin film. The fwhm measured was ~0.12°, which suggests the high quality, nearly single crystalline nature of the film. The fwhm measured for the substrate was 0.02° (not shown here).
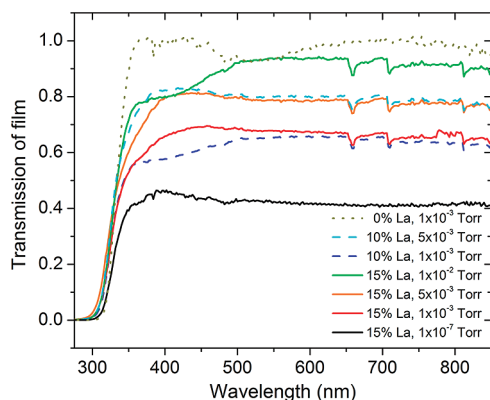

Figure 3. Transmission of various 150 nm double-doped STO films on LSAT substrate over the UV−visible part of the electromagnetic spectrum. Apart from the transparent conducting films, the plots for the insulating (0% La grown at 10^{-3} Torr) and nontransparent but conducting (15% La grown at 10^{-7} Torr) films are also shown for comparison.

the whole UV−visible range of the electromagnetic spectrum is shown in Figure 3. The figure clearly shows the transparent nature of the films with either 10 or 15% La doping grown in the pressures ranging from 10^{-2} to 10^{-3} Torr. The transmission of the films with 15% La grown at 10^{-7} Torr (Figure 1c) and no La doping grown at 10^{-3} Torr (Figure 1a) are shown as comparison. As shown in Figure 1, the nontransparent conducting samples shows much lower transmission compared to the transparent

conducting and insulating films. The insulating film showed the maximum possible transmission over the whole range of the spectrum. Tauc plot of the films showed that the indirect band gap of the films was ~3.2−3.3 eV for all the doping levels, very similar to the bulk indirect gap of 3.27 reported in the literature.[19]

Figure 4b depicts the measured sheet resistance of the TCO films as a function of transmission of the film at 600 nm. A logarithmic scaling behavior was observed between the sheet resistance and transmission. The growth pressure influenced the sheet resistance or transmission more than the La doping, emphasizing the role of the oxygen vacancies in forming the defect band below the conduction band. The resistivity, carrier concentration, and mobility of the 15% La doped film grown at 10^{-3} Torr as a function of temperature are shown in Figure 4a. The resistivity fit indicated the presence of small polaron conduction mechanism as reported in the literature.[20] The small polaron equation used for the fitting is shown in eq 1.

$$\rho \sim \sinh^2\left(\frac{A}{T}\right) \qquad (1)$$

It is interesting to note that the sample remains metallic throughout the temperature range, implying degenerate

(19) Capizzi, M.; Frova, A. *Phys. Rev. Lett.* **1970**, *25*, 1298.
(20) Liang, S.; Wang, D. J.; Sun, J. R.; Shen, B. G. *Solid State Commun.* **2008**, *148*, 386.
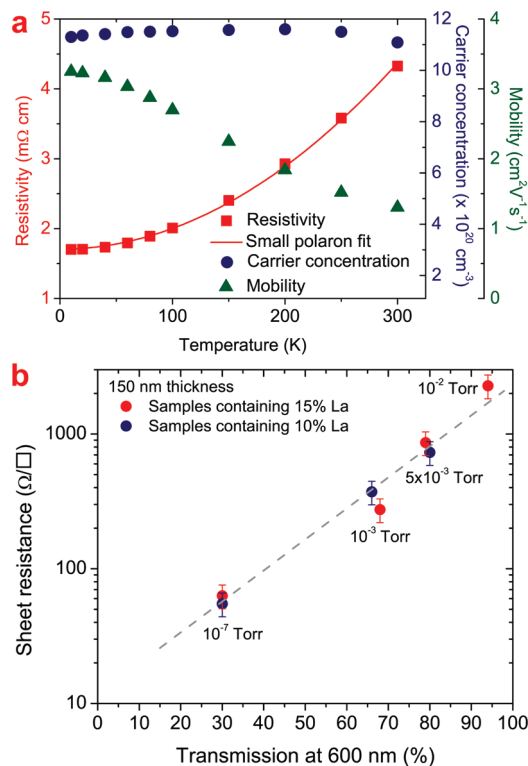
Figure 4. (a) Resistivity, Hall carrier concentration, and Hall mobility of the transparent conducting film with 15% La doping and grown at 10^{-3} Torr. The red line is the small polaron fit for the resistivity. (b) Sheet resistance of various transparent conducting films against their transmission for an incident radiation with a wavelength of 600 nm. The dashed line is a logarithmic fit.

doping. Hall measurements and thermopower measurements (not shown here) revealed electrons as the major transport carriers irrespective of the dopant (La or oxygen vacancies). Due to the small polaron behavior, double-doped STO has very low mobility ($1-5$ cm^2 V^{-1} s^{-1}) compared to conventional TCOs like Sn doped In$_2$O$_3$ (ITO), Nb doped TiO$_2$, and Al doped ZnO (AZO), which have much larger mobilities ($\sim$100 cm^2 V^{-1} s^{-1}). This also leads to much larger sheet resistances ($\sim$100$-$1000 Ω/□) as compared to lower sheet resistances for conventional TCOs ($1-100$ Ω/□) for similar transparency.[21]

To confirm the role of oxygen vacancies in forming the defect band, we performed optical spectroscopic measurements, in this case, photoluminescence (PL) and UV−visible (UV−vis) absorption. These measurements provide information about the optical band structure of the material; PL and UV−vis absorption provide information about the in-gap states and band edges, respectively. The typical Tauc plot derived from UV−vis absorption and the PL spectra for 15% La doped sample grown at 10^{-3} Torr are shown in Figure 5. The PL spectrum shows a peak at ~420 nm, which indicates the presence of an oxygen vacancy defect band, approximately 2.9 eV above the valence band, as reported elsewhere.[22] Figure 5c summarizes the optical band

(21) Gordon, R. G. *MRS Bull.* **2000**, *25*(8), 52.
(22) Mochizuki, S.; Fujishiro, F.; Minami, S. *J. Phys.: Condens. Matter* **2005**, *17*, 923.
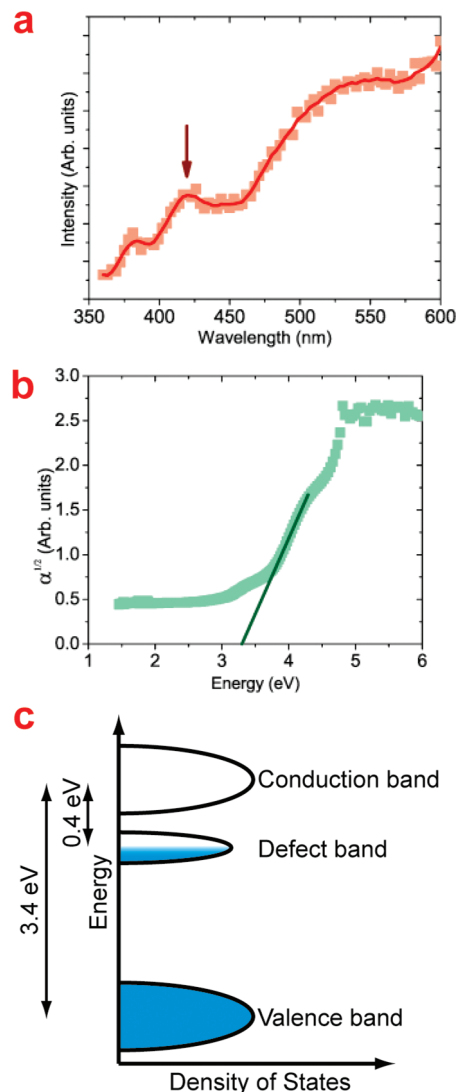
Figure 5. (a) PL spectrum for 15% La doped film grown at 10^{-3} Torr. The red arrow indicates the peak corresponding to the oxygen vacancy defect band ($\sim$ 420 nm). (b) Tauc plot for the same sample. The derived optical indirect band gap is 3.3 eV. (c) Schematic of the optical band structure derived for the transparent conducting films. The chemical potential lies in the defect band, which is crucial for a transparent conductor.

structure as mapped by these spectroscopic techniques for the TCO samples.

Conclusion

In summary, we have demonstrated a transparent conducting oxide in double-doped STO over a range of doping levels. Based on the optical band structure and transport measurements, we substantiate the formation of a defect band due to the oxygen vacancies. This defect band is the most important component of the guiding principle behind TCO formation, as discussed earlier. The filling of this band can be accurately controlled by varying both the La doping and the oxygen partial pressure during growth to produce a controlled TCO in the double-doped STO. Double-doped STO can be used in conjugation with a wide range of complex

oxides, particularly perovskite oxides for the demonstration of various opto-electronic and photonic devices. This work also emphasizes the versatility of STO, a model oxide system, capable of showing myriad properties relevant for various technological applications.